Inorganic Chemistry
Article

Inorg. Chem. **2010**, *49*, 1667–1673 **1667**
DOI: 10.1021/ic902058n

Stacked Nickelocenes: Synthesis, Structural Characterization, and Magnetic Properties

Sabrina Trtica, Marc Heinrich Prosenc,* Michael Schmidt and Jürgen Heck*

Institute of Inorganic and Analytical Chemistry, University of Hamburg, Martin-Luther-King-Platz 6, 20146 Hamburg, Germany

Ole Albrecht and Detlef Görlitz

Institute of Applied Physics and Microstructure Research Centre, University of Hamburg, Jungiusstrasse 11, 20355 Hamburg, Germany

Frank Reuter and Eva Rentschler

Institute of Inorganic and Analytical Chemistry, Johannes Gutenberg University of Mainz, Duesbergweg 10-14, 55128 Mainz, Germany

Received October 17, 2009

The disubstitution of 1,8-diiodonaphthalene (**1**) with cyclopentadienyl nucleophiles reveals 1,8-(dicyclopentadienyl)-naphthalene, which rapidly undergoes Diels−Alder reaction forming 1,8-(3a′,4′,7′,7a′-tetrahydro-4′,7′-methanoindene-7a′,8′-diyl)-naphthalene (**2**). A subsequent retro-Diels−Alder reaction in the presence of sodium hydride yields the disodium salt of 1,8-(dicyclopentadiendiyl)-naphthalene **3**. The disodium salt **3** was the starting material to obtain the paramagnetic bisnickelocene derivative **4**, which structure was obtained by X-ray structure analysis, revealing two nickelocenes kept together in a stacked fashion by a 1,8-naphthalene clamp. An electronic interaction between the two nickel atoms is found as a result of cyclic voltammetry, indicating five different oxidation states +4, +3, +2, +1, and 0. The magnetic properties of **4** in solution were studied by variable temperature paramagnetic ^{1}H NMR spectroscopy and Evans method and revealed Curie behavior between 213 and 293 K. The magnetic susceptibility of a powdered sample of **4** was measured, and an antiferromagnetic interaction with an exchange coupling of $J_{12} = -31.49$ cm^{-1} is found. In accord with experimental data, broken symmetry density functional theory (DFT) calculations revealed four antiferromagnetically coupled electrons resulting in an open shell singlet ground state.

Introduction

Di- and polynuclear aggregates of paramagnetic metallocenes are interesting building blocks for materials expected to exhibit interesting magnetic properties.[1] The synthesis of molecular based magnetic materials has been pursued by many groups over the past decade.[2] The aim is to arrange the paramagnetic centers in such a way that the interactions of spins result in spontaneous magnetization. Organic radicals, open-shell transition metal ions, and a combination of both are used to design these materials. Pure organic polyradicals are less advantageous because of their reactivity in contrast to metal centered radicals as in paramagnetic coordination compounds and organometallic examples.[3,4]

*Corresponding author. E-mail: juergen.heck@chemie.uni-hamburg.de (J.H.); prosenc@chemie.uni-hamburg.de (M.H.P.). Phone: 0049/(0)40/428386375 (J.H.); 0049/(0)40/428383102 (M.H.P.). Fax: 0049/(0)40/428386945 (J.H.); 0049/(0)40/428382882 (M.H.P.).

(1) (a) Barlow, S.; O'Hare, D. *Chem. Rev.* **1997**, *97*, 637–670. (b) Altmannshofer, S.; Herdtweck, E.; Köhler, F. H.; Miller, R.; Mölle, R.; Scheidt, E.-W.; Scherer, W.; Train, C. *Chem.—Eur. J.* **2008**, *14*, 8013–8024. (c) Rosenblum, M. *Adv. Mater.* **1994**, *6*(2), 159–162. (d) Atzkern, H.; Bergerat, P.; Beruda, H.; Fritz, M.; Hiermeier, J.; Hudeczek, P.; Kahn, O.; Köhler, F. H.; Paul, M.; Weber, B. *J. Am. Chem. Soc.* **1995**, *117*, 997–1011. (e) Astruc, D. *Acc. Chem. Res.* **1997**, *30*, 383–391. (f) Hilbig, H.; Hudeczek, P.; Köhler, F. H.; Xie, X.; Bergerat, P.; Kahn, O. *Inorg. Chem.* **1998**, *37*, 4246–4257.

(2) (a) Kahn, O. *Acc. Chem. Res.* **2000**, *33*, 647–657. (b) Miller, J. S.; Epstein, A. J. *MRS Bull.* **2000**, *25*(11), 21–28. (c) Epstein, A. J. *MRS Bull.* **2000**, *25*(11), 33–40. (d) Veciana, J.; Iwamura, H. *MRS Bull.* **2000**, *25*(11), 41–51. (e) Awaga, K.; Coronado, E.; Drillon, M. *MRS Bull.* **2000**, *25*(11), 52–57. (f) Miller, J. S. *MRS Bull.* **2000**, *25*(11), 60–64. (g) Christou, G.; Gatteschi, D.; Hendrickson, D. N.; Sessoli, R. *MRS Bull.* **2000**, *25*(11), 66–71. (h) Verdaguer, M. *Polyhedron* **2001**, *20*(11−14), 1115–1128. (i) Miller, J. S. *MRS Bull.* **2007**, *32*, 549–555. (j) Veciana, J.; Cirujeda, J.; Rovira, C.; Vidal-Gancedo, J. *Adv. Mater.* **1995**, *7*(2), 221–225.

(3) Miller, J. S.; Epstein, A. J. *Angew. Chem., Int. Ed. Engl.* **1994**, *33*, 385–415.

Published on Web 01/19/2010

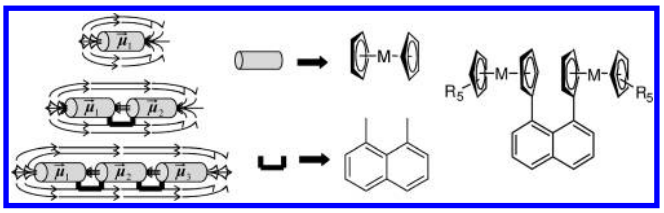

Figure 1. Head-to-head stacked, paramagnetic metallocenes supposed as molecular bar magnets.

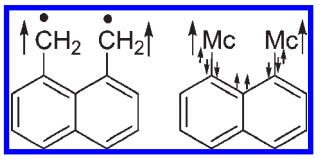

Figure 2. Two single electrons in α-positions of a 1,8-disubstituted naphthalene[8] (left). A sequence of spin polarization via σ-bonds leading to a ferromagnetic interaction between unpaired electrons of paramagnetic metallocenes (Mc) in the 1,8-position of naphthalene[3,9] (right).

Our target to build up molecular based magnetic materials is to stack paramagnetic metallocenes in a head-to-head fashion, which may lead to molecular bar magnets. This approach has its macroscopic counterpart in a one-dimensional stacking of small bar magnets resulting in an increased magnetic anisotropy (Figure 1, left).

In order to stack two paramagnetic nickelocenes, we applied the method of a 1,8-naphthalene clamp (Figure 1, right) developed by Rosenblum and co-workers for diamagnetic congeners,[5] and it has been extended to dipolar[6] and paramagnetic[7] complexes.

From organic compounds containing substituents with two unpaired electrons in the 1,8-position of naphthalene, it is well-known that a triplet state ($S = 1$) is closely above (188 J/mol) the singlet ground state ($S = 0$)[8] (Figure 2, left). Considering spin polarization along the naphthalene backbone as one mechanism for the magnetic communication between two paramagnetic centers in the 1,8-position of naphthalene, the unpaired electrons should even be ferromagnetically coupled[9] (Figure 2, right). Another pathway of magnetic interaction could be due to spin-polarization effects via the adjacent π-orbitals of face-to-face stacked paramagnetic sandwich complexes, such as proposed for the paramagnetic 1,8-bis-(trovacenyl)-naphthalene, which leads to an antiferromagnetic coupling.[7a] A third mechanism may be a dipolar "through-space" coupling between the paramagnetic centers, which depends strongly on the distance between the paramagnetic centers. Therefore, it would be most interesting to gain a deeper understanding of the magnetic interactions in one-dimensionally aligned paramagnetic metallocenes. In this paper we want to present the first synthesis of a head-to-head stacked bisnickelocene linked together by a naphthalene clamp and results of magnetic behavior.

Scheme 1. Synthesis of the Bisnickelocene Complex **4**

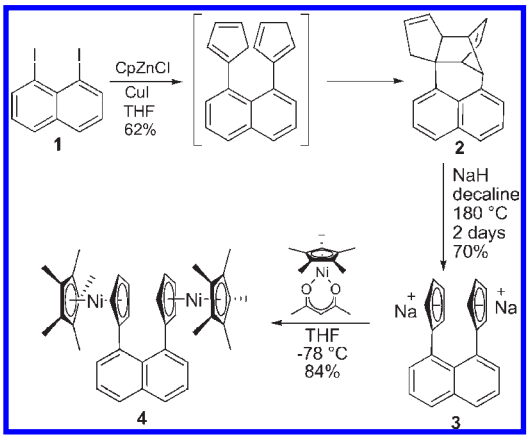

Results and Discussion

Synthesis. For the synthesis of the target compound (**4**) 1,8-diiodonaphthalene (**1**) was taken as the starting material, which was subjected to a cross-coupling reaction with cyclopentadienyl zinc chloride in the presence of copper iodide (Scheme 1). It results in the formation of 1,8-(dicyclopentadienyl)-naphthalene, which was not isolated but readily underwent a Diels−Alder reaction to obtain compound **2**.[6b] The hydrocarbon **2** was characterized by X-ray structure analysis,[6b] and the molecular structure confirms the geometry proposed by Rosenblum et al.[5d] The second step was a retro-Diels−Alder reaction, performed in decaline at 180 °C in the presence of sodium hydride yielding back the 1,8-(dicyclopentadienyl)-naphthalene, which immediately transforms into the disodium salt of 1,8-(dicyclopentadiendiyl)-naphthalene **3**. The sodium salt **3** was transferred to the target bisnickelocene complex **4** by adding [NiCp*(acac)][10] which was used as an effective NiCp*-transfer reagent.

Molecular Structure of the Bisnickelocene Complex 4. Complex **4** was obtained in dark-red crystals from a hexane solution in a sufficient quality for X-ray structure analysis. It crystallizes in the triclinic space group $P\bar{1}$ with two independent molecules in the asymmetric unit. The molecules demonstrate a distorted structure caused by nonbonding repulsions of the two head-to-head stacked nickelocene units in the peri position of the naphthalene "backbone" of **4**. Similar features have been reported on related naphthalene derivatives substituted in the peri

(4) (a) Bachmann, B.; Heck, J.; Meyer, G.; Pebler, J.; Schleid, T. *Inorg. Chem.* **1992**, *31*, 607–614. (b) Hermans, P. M. J. A.; Scholten, A. B.; van der Beuken, E. K.; Bussaard, H. C; Roeloffsen, A.; Metz, B.; Reijerse, E. J.; Beurkens, P. T; Bosman, W. P; Smith, J. M. M.; Heck, J. *Chem. Ber.* **1993**, *126*, 553–563. (c) Heck, J.; Hermans, P. M. J. A.; Scholten, A. B; Bosmann, W. P. J. H.; Meyer, G.; Staffel, T.; Stürmer, R.; Wünsch, M. *Z. Anorg. Allg. Chem.* **1992**, *611*, 35–42. (d) Behrens, U.; Heck, J.; Maters, M.; Frenzen, G.; Roelofsen, A.; Sommerdijk, H. T. *J. Organomet. Chem.* **1994**, *475*, 233–240. (e) Gatteschi, D. *Adv. Mater.* **1994**, *6*(9), 635–645. (f) Manriquez, J. M.; Ward, M. D.; Reiff, W. M.; Calabrese, J. C.; Jones, N. L.; Corroll, P. J.; Brunel, E. E.; Miller, J. S. *J. Am. Chem. Soc.* **1995**, *117*, 6182–6193.

(5) (a) Rosenblum, M.; Nugent, H. M.; Jang, K. S.; Labes, M. M.; Cahalane, W.; Klemarczyk, P.; Reiff, W. M. *Macromolecules* **1995**, *28*, 6630–6342. (b) Hudson, R. D. A.; Foxman, B. M.; Rosenblum, M. *Organometallics* **1999**, *18*, 4098–4106. (c) Hudson, R. D. A.; Foxman, B. M.; Rosenblum, M. *Organometallics* **2000**, *19*, 469–474. (d) Foxman, B. M.; Gronbeck, D. A.; Khruschova, N.; Rosenblum, M. *J. Org. Chem.* **1993**, *58*, 4078–4082. (e) Arnold, R.; Foxman, B. M.; Rosenblum, M. *Organometallics* **1988**, *7*, 1253–1259.

(6) (a) Malessa, M.; Heck, J.; Kopf, J.; Garcia, M. H. *Eur. J. Inorg. Chem.* **2006**, 857–867. (b) Werner, M. PhD Thesis, Dipolar gestapelte Sandwich-Komplexe als potenzielle NLO Chromophore,University of Hamburg, **2009**.

(7) (a) Elschenbroich, C.; Wolf, M.; Schiemann, O.; Harms, K.; Burghaus, O.; Pebler, J. *Organometallics* **2002**, *21*, 5810–5819. (b) Pagels, N.; Heck, J. *J. Organomet. Chem.* **2008**, *693*, 241–246.

(8) (a) Pagni, R. M.; Burnett, M. N.; Dodd, J. R. *J. Am. Chem. Soc.* **1977**, *99*, 1972–1973. (b) Muller, J.-F.; Muller, D.; Dewey, H. J.; Michl, J. *J. Am. Chem. Soc.* **1978**, *100*, 1629–1630.

(9) Gerson, F.; Huber, W. *Electron Spin Resonance Spectroscopy of Organic Radicals*; Wiley-VCH: Weinheim, 2003.

(10) Bunel, E. E.; Valle, L.; Manriquez, J. M. *Organometallics* **1985**, *4*, 1680–1682.

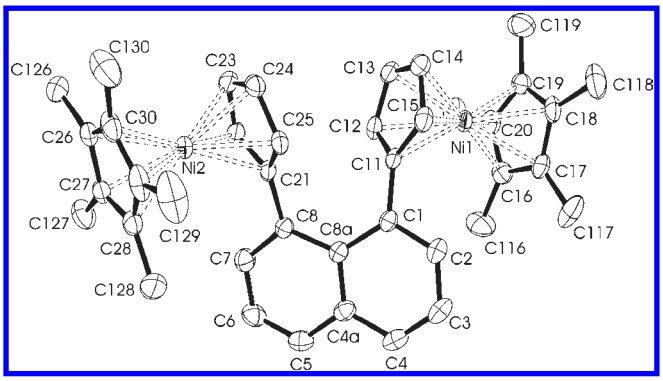

Figure 3. ORTEP plot of the molecular structure of **4** (hydrogen atoms are omitted for clarity; displacement ellipsoids are drawn at the 50% probability level).

position with two sandwich complexes (Figure 3).[5e,6,7] The torsion angle between the bonds of C(1)−C(11) and C(8)−C(21) amounts to 27.5° (Figure 3, Table 1). The tilt angle between the best plane of the naphthalene-bound Cp ligands and the best plane of the connected six-membered naphthalene rings is about 42.9° and 42.4°, respectively. The Ni(1)−C(11) and Ni(2)−C(21) bond lengths are significantly longer (223.1(2) and 225.5(2) pm, respectively) than the other Ni−C(Cp) distances which vary between 215.4(2) and 220.2(2) pm (Table 1). The slightly slipped fashion of the cyclopentadienyl ligand also holds for the Cp* ligand although symmetrically substituted and was already mentioned by Dunitz and Seiler.[11] The molecular structure of the nickelocene subunits in complex **4** is very similar to the structure of other nickelocene derivatives.[11]

A remarkable feature of the crystalline state of complex **4** is the one-dimensional stacking of the single bis-sandwich units forming a columnar alignment throughout the whole crystal. The columns are parallel ordered (Figure 4). Most interestingly, the intramolecular nickel−nickel distance is about 697.1(1) pm, whereas the shortest intermolecular nickel−nickel distance is only about 44 pm longer (741.3(1), Figure 4).

DFT Calculations. In order to gain deeper insight into the electronic structure of the bisnickelocene complex **4**, quantum chemical calculations were performed using the density functional theory (DFT) method, which has been successfully employed on calculations of related systems.[12] Initial optimization of complex **4** revealed a nearly C_2-symmetric structure. Thus, for further calculations C_2-symmetry has been imposed. A relaxation of the initial wave function revealed a quintet ground state (^{5}A in C_2-symmetry) for the model system which is in agreement with previously published data[12,13] in which a triplet ground state was found for one nickelocene fragment ($^3A_1'$). Geometry optimization of **4** in a quintet state leads to geometry parameters listed in Table 1. Distances to the centroid of the five membered rings of Ni−Cent (186.1 and 181.9 pm) and distances of Ni−C of 218.0−220.2 pm (Cp*), Ni−C of 214.3−233.2 (C_5H_4) and C_{ipso}−C_{ipso}

Table 1. Selected Angles (deg) and Bond Lengths (pm) of **4** Obtained by X-ray Structure Analysis and by Means of Density Functional Theory (DFT) Calculations

	X-ray structure	DFT calculations
C(11)−C(1)−C(8)−C(21)	27.5(2)	32.3
C(1)−C(11)	148.2(3)	147.0
C(8)−C(21)	147.8(3)	147.0
C(1)−C(8)	256.2(3)	257.5
C(11)−C(21)	299.0(3)	309.1
Ni(1)−Ni(2)	697.1(1)	715.3
$Cent_{[C(11)-C(15)]}$−$Cent_{[C(16)-C(20)]}$[a]	363.7(1)	369.5
$Cent_{[C(11)-C(15)]}$−$Cent_{[C(21)-C(25)]}$[a]	351.7(1)	368.0
$Cent_{[C(21)-C(25)]}$−$Cent_{[C(26)-C(30)]}$[a]	362.9(1)	369.5
Ni−C ($C_5(CH_3)_5$)	214.6−220.4	218.0−220.2
Ni−C_{ipso}(C_5H_4)	222.7−225.5	233.2
Ni−C_α (C_5H_4)	219.0−220.2	224.9, 222.5
Ni−C_β (C_5H_4)	215.4−217.4	216.1, 214.3
Cent−Ni−Cent	174.5−177.0	178.4
Ni−Cent	179.9−183.4	186.1, 181.9

[a] Cent: centroid of the corresponding Cp ligand.

(C(11)−C(21)) of 309.1 pm are in good agreement with structural parameters obtained by X-ray structure analysis. In agreement with the almost 5-fold symmetry of the nickelocene unit, calculation of the frontier orbital structure reveals four nearly degenerate single occupied molecular orbitals. Due to a weak overlap between the C(11), C(21) carbon atoms (Figure 5), the four molecular orbitals split into two sets of nearly degenerate singly occupied orbitals (Figure 5). To determine the electronic ground state, broken symmetry calculations were performed, revealing a singlet ground state calculated to be 3 kJ/mol less in energy than the quintet state.

The calculation of the electronic structure gained the lowspin state to be more stable than the highspin state. For an analysis of the wave function, initially three mechanisms were taken into account. First, a spin polarization mechanism via the naphthalene bridge, which would lead to a ferromagnetic coupling. The dipolar interaction can be neglected due to the large distance between the paramagnetic centers. However, the calculations revealed an interaction of the paramagnetic centers through the stacked π-systems of the nickelocene subunits and along the π-system of the naphthalene bridge.

In order to elucidate the interaction between the paramagnetic centers, the electronic structure of complex **4** was analyzed. From Figure 5, it can be deduced that the highest two degenerate singly occupied molecular orbitals exhibit orbital coefficients not only on the metallocene fragment but also on the π-system of the naphthalene bridge. The overlap between the nickelocene and the bridge is nonzero and thus, the coupling through the ligand results in a superexchange interaction between the two nickelocene spin orbitals leading to an antiferromagnetic coupling between the unpaired electrons.

In addition, a superexchange might occur by a direct interaction between the adjacent two Cp ligands of the nickelocene subunits. From the second highest single occupied degenerate molecular orbitals, the exchange mechanism between the spin orbitals of the two nickelocene fragments differ from the interaction above-discussed, due to the lack of overlap between the nickelocene and the naphthalene π-orbitals. Spin polarization might be here

(11) Seiler, P.; Dunitz, J. D. *Acta Crystallogr.* **1980**, *B36*, 2255–2260.
(12) Hrobárik, P.; Reviakine, R.; Arbuznikov, A. V.; Malkina, O. L.; Malkin, V. G.; Köhler, F. H.; Kaupp, M. *J. Chem. Phys.* **2007**, *126*, 024107.
(13) Xu, Z. F.; Xie, Y.; Feng, W.-L.; Schaefer, H. F. *J. Phys. Chem. A* **2003**, *107*, 2716–2729.

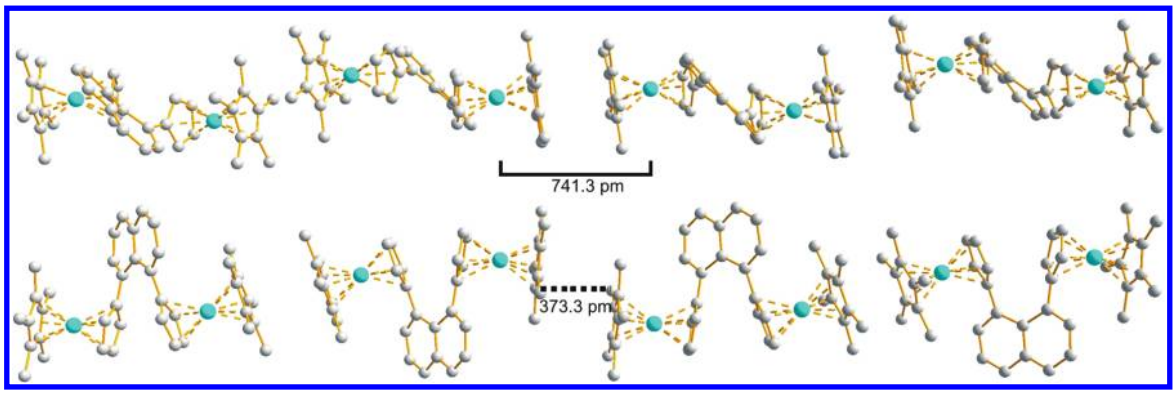

Figure 4. DIAMOND plot: Columnar packing of molecules of complex **4** in the crystalline state illustrating the head-to-head stacked intermolecular arrangement of the metallocene units. The lower column is the same as the upper one turned by 90°.

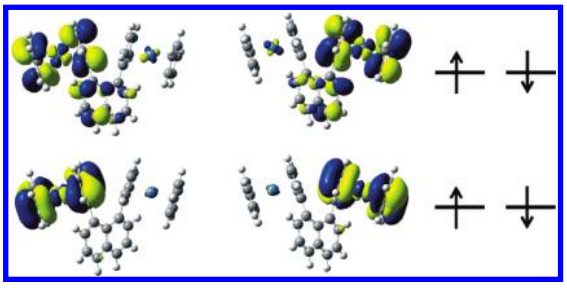

Figure 5. Highest single occupied molecular orbitals. The bonding and antibonding interaction of the linking C_5 rings results in a splitting of the two degenerate orbitals. The CH_3 substituents are omitted for clarity.

triggered by "through-space" interactions between the two nickelocene fragments mediated by lower lying orbitals.

To gain deeper insight into the nature of this "through-space" interaction, we calculated the electronic structure of the two nickelocene units without the naphthalene bridge (the former naphthalene bound C-atoms of Cp ligands were saturated by hydrogen atoms) in the same geometric arrangement. The calculation also revealed a singlet electronic ground state. The singlet-quintet gap is calculated to be 3.7 kJ/mol, which is slightly higher in energy than in the bridged complex **4**. Thus, two different spin−spin interaction paths by superexchange appear to be responsible for the singlet ground state being lower in energy in complex **4** than a triplet or quintet state. The size of the antiferromagnetic interactions in the bridged complex **4** is slightly reduced by a ferromagnetic spin polarization through the bridge.

Redox Properties. The redox chemistry of the bisnickelocene derivative **4** has been investigated by means of cyclic voltammetry (Figure 6). The cyclic voltammogram of **4** in THF displays four redox couples with potentials in the range of pentamethylnickelocene.[14] The redox couples appear in two pairs of a large separation of about 1 V, which is typical for nickelocenes, and each pair of the only partly resolved redox couples is separated by $\Delta E_{1/2}(2-1) = 0.128$ V, $\Delta E_{pa}(4-3) = 0.158$ V, respectively (Table 2), demonstrating a weak metal−metal interaction. With regard to the electrochemical results of nickelocene[15] and the pentamethylated derivative,[14] the redox couples are caused by four one electron transfers resulting in five

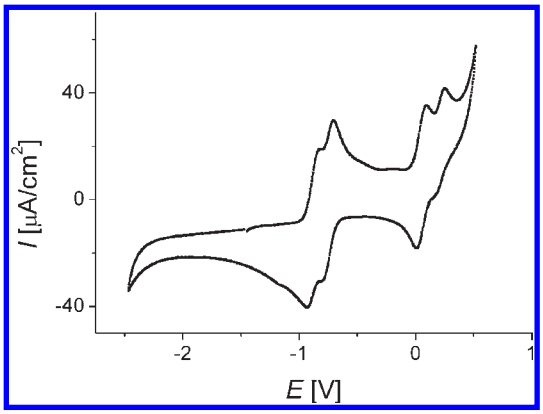

Figure 6. Cyclic voltammogram of **4**.

Table 2. Cyclic Voltammetry Data[a] of **4**

redox couples	$E_{1/2}$[b]	E_{pa}	E_{pc}	ΔE_p[c]		
0/+1	−0.877	−0.827	−0.927	0.100	$\Delta E_{1/2}(2-1)$[d]	0.128
+1/+2	−0.749	−0.706	−0.792	0.086	$\Delta E_{pa}(4-3)$[e]	0.158
+2/+3	0.053	0.094	0.011	0.083	$\Delta E_{1/2}(3-1)$[d]	0.930
+3/+4		0.252			$\Delta E_{pa}(4-2)$[e]	0.958

[a] In THF at room temperature, $[n\text{Bu}_4\text{N}]\text{PF}_6$ (0.4 M) as the supporting electrolyte, Pt as the standard electrode referenced vs $E_{1/2}$(ferrocene/ferrocenium) = 0 V, scan rate 300 mV/s. Potentials E in volts ±0.005 V. [b] $E_{1/2} = (E_{pa} + E_{pc})/2$. [c] $\Delta E_p = |E_{pc} - E_{pa}|$. [d] $\Delta E_{1/2}(2-1) = |E_{1/2}(2) - E_{1/2}(1)|$. [e] $\Delta E_{pa}(4-3) = |E_{pa}(4) - E_{pa}(3)|$.

Scheme 2. Redox Cascade for the Bisnickelocene Compound **4**

$$[\text{Ni/Ni}] \underset{E_{1/2}(1)}{\overset{e^-}{\rightleftharpoons}} [\text{Ni/Ni}]^{+} \underset{E_{1/2}(2)}{\overset{e^-}{\rightleftharpoons}} [\text{Ni/Ni}]^{2+} \underset{E_{1/2}(3)}{\overset{e^-}{\rightleftharpoons}} [\text{Ni/Ni}]^{3+} \xrightarrow[E_{pa}(4)]{e^-} [\text{Ni/Ni}]^{4+}$$

different oxidation states (+4, +3, +2, +1, and 0) (Scheme 2). According to the redox properties of the parent nickelocenes,[14,15] the first and the second oxidation steps seem to be electrochemically reversible whereas the third redox couple $E_{1/2}(3)$ is only partially reversible and the fourth one $E_{pa}(4)$ is presumably chemically irreversible.

Magnetic Measurements. The magnetic behavior of **4** in solution was investigated by variable temperature ^{1}H NMR (Figure 7). The chemical shift of the methyl groups ($\delta_{para,293}$ = 202.5 ppm) and of H 2′/5′, H 3′/4′ ($\delta_{para,293}$ = −162.9 ppm, $\delta_{para,293}$ = −173.4 ppm) are much larger than found for the decamethylated fulvalene bridged dinickelocene[16] published

(14) Hudeczek, P.; Köhler, F. H.; Bergerat, P.; Kahn, O. *Chem.—Eur. J.* **1999**, *5*(1), 70–78.
(15) Chong, D.; Slote, J.; Geiger, W. E. *J. Electroanal. Chem.* **2009**, *630* (1−2), 28–24.
(16) Hudeczek, P.; Köhler, F. H. *Organometallics* **1992**, *11*, 1773–1775.

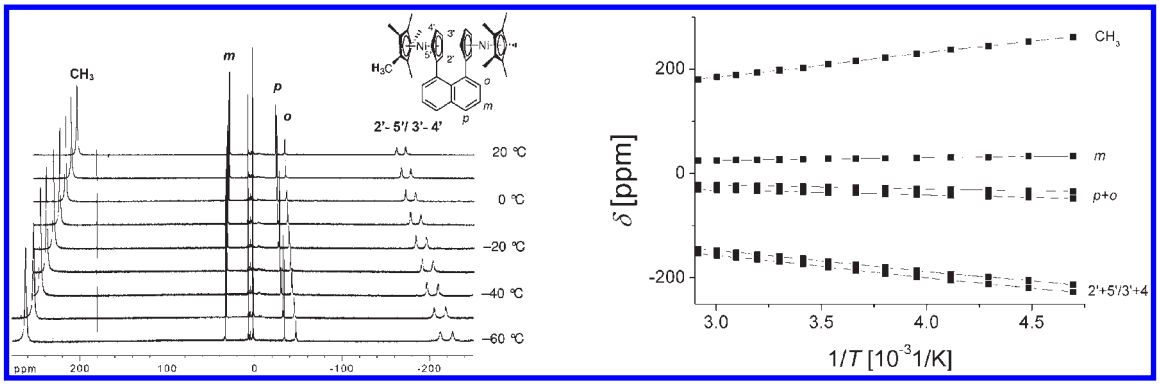

Figure 7. (left) ^{1}H NMR spectra of **4** in toluene-d_8 recorded at different temperatures. The signal shifts were measured relative to the solvent signal. (right) Curie plot of the chemical shift δ versus reciprocal temperature.

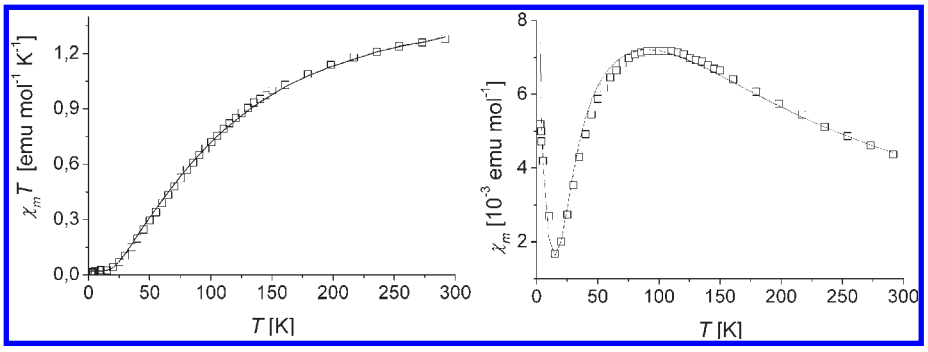

Figure 8. Magnetochemical behavior of complex **4**. Solid lines represent the best theoretical fit: (left) $\chi_m T$ vs temperature; (right) χ_m vs temperature.

by Köhler and co-workers ($\delta_{para,298}$ = 117.9, and −122.1/−100.6 ppm), which may be due to stronger antiferromagnetic coupling in the decamethylated fulvalene bridged dinickelocene compared to the head-to-head stacked congeners described in this paper (vide supra). However the extension of the chemical shifts in **4** are still smaller than found for the unsubstituted pentamethylnickelocene ($\delta_{para,298}$ = 233, −210 ppm), thus indicating an interaction between the nickelocene units.

The VT ^{1}H NMR spectra (Figure 7, right) demonstrates a linear correlation between the chemical shift of the proton resonance signals of **4** and the reciprocal temperature. The linear slope proves a Curie behavior in the temperature range of $-60 < T < 20$ °C. In accordance with the Curie behavior of **4** in solution is the magnetic moment μ_{eff}, which was determined to 3.60 μ_B by ^{1}H NMR with the Evans method.[17] The effective magnetic moment μ_{eff} = 3.60 μ_B confirms a spin state of two times $S = 1$, thus four unpaired electrons as expected. In order to obtain more information about the magnetic behavior of **4**, the susceptibility of a micro crystalline sample was determined by variable temperature magnetic measurements in the temperature range of 2−300 K (Figure 8).

Experimental susceptibility data were corrected for the underlying diamagnetism with Pascal's constants.[18] The $\chi_m T$ versus T curve (Figure 8, left) decreases as the temperature is lowered. The χ_m versus T curve (Figure 8, right) shows a rounded maximum at about 101 K, which is characteristic for an antiferromagnetic interaction. The magnetic moment μ_{eff} (calculated from χ_m data) is equal to 3.20 μ_B at room temperature, which is less than expected for two isolated local spins of $S_{Ni} = 1$ ($\mu_{eff} = 4\,\mu_B$ at room temperature for $S_1 = S_2 = 1$ and $g = 2$, using the spin-only approximation).[3] Using the spin Hamiltonian $\hat{H} = -2J_{ij}\sum\hat{S}_i \cdot \hat{S}_j$, the susceptibility data could be simulated satisfactory with $\hat{S}_1 = \hat{S}_2 = 1$, $J_{12} = -31.49$ cm^{-1}, $\Theta = 1.40$ K and $g_1 = g_2 = 1.813$. An additional small paramagnetic impurity of 2.1% has to be taken in account. The g-value less than 2.0 is in accordance with values reported for nickelocene and pentamethylnickelocene.[19] This result confirms a weak intramolecular antiferromagnetic interaction mainly by strong $\pi-\pi$ interaction due to the stacking of the naphthalene bound Cp units with shortest contacts found at 299.0 pm for C(11)−C(21) (Figure 3, Table 1). The small Θ value $\neq 0$ gives an indication for some intermolecular interaction mediated by $\pi-\pi$ interaction of two adjacent Cp* ligands, the shortest distance being 373.3 pm (Figure 4).

Conclusion

A synthetic route to head-to-head stacked paramagnetic nickelocenes has been demonstrated started with 1,8-diiodonaphthalene. The substitution of the diiodo functions with cyclopentadienyl substituents yields a Diels−Alder product **2**. In a subsequent retro-Diels−Alder reaction in the presence of sodium hydride, the dianion 1,8-(dicyclopentadiendiyl)-naphthalene **3** was formed. Upon addition of a NiCp*-transfer reagent, the paramagnetic target complex

(17) Evans, D. F. *J. Chem. Soc.* **1959**, 2003–2005.
(18) Bain, G. A.; Berry, J. F. *J. Chem. Educ.* **2008**, *85*(4), 532–536.
(19) (a) Castellani, M. P.; Geib, S. J.; Rheingold, A. L.; Trogler, W. C. *Organometallics* **1987**, *6*, 1703–1712. (b) Robbins, J. L.; Edelstein, N.; Spencer, B.; Smart, J. C. *J. Am. Chem. Soc.* **1982**, *104*, 1882–1893.

1,8-bis[(η^5-pentamethylcyclopentadienyl)(η^5-cyclopentadiendiyl)nickel(II)]-naphthalene (**4**) was obtained.

The X-ray structure analysis of **4** revealed a head-to-head arrangement of the two nickelocene units linked together by a 1,8-naphthalene clamp.

DFT calculations of the electronical structure of complex **4** revealed a singlet ground state with a low above lying quintet state. Geometrical optimization of **4** is in good agreement with structural parameters obtained by X-ray structure analysis.

In a cyclic voltammetry study of **4**, two well-separated pairs of redox couples can be observed which separation is in accordance to the electrochemical behavior of the mononuclear parent nickelocenes. The appearance of the redox couples in pairs is caused by the successive oxidation and rereduction of the two nickelocene centers closely connected indicating a weak metal−metal interaction.

Paramagnetic variable temperature ^{1}H NMR experiments point out a Curie behavior of the two nickelocenes in solution between 293 and 213 K. The application of Evans method revealed a magnetic moment for a spin state of two times $S = 1$ in solution, thus two unpaired electrons on each Ni center in **4**. Bulk susceptibility measurements reveal an antiferromagnetic interaction with an exchange coupling of $J_{12} = -31.49\ cm^{-1}$. This result is in agreement with the calculations by means of DFT methods illustrating in a singlet ground state of **4**. In addition, the DFT calculations reveal two different superexchange pathways of electron spin-spin coupling responsible for the singlet ground state. Measurements of solved magnetically diluted samples are planned, which should enable us to discriminate between an intra- and intermolecular magnetic interaction. The latter may contribute distinctly to the magnetic interaction, since the intramolecular metal−metal distance is only about 44 pm shorter than the intermolecular one.

Experimental Section

General. Unless otherwise noted, the reactions were carried out under dry nitrogen using standard Schlenk technique. Solvents were saturated with nitrogen. Tetrahydrofuran (THF) and *n*-hexane were dried by sodium potassium alloy. 1,8-Diiodonaphthalene[20] (**1**) and (acetylacetonato)(η^5-pentamethylcyclopentadienyl)nickel(II) [NiCp*(acac)][10] were synthesized according to literature procedures. The anhydrous zinc chloride ($ZnCl_2$) was dried with thionyl chloride, and the THF adduct was prepared by refluxing the water free $ZnCl_2$ in THF. Cyclopentadienyl lithium (LiCp) was synthesized from a 1.6 M solution of *n*-butyllithium in hexane with freshly cracked cyclopentadiene in hexane. The white precipitate was filtered and dried under vacuum. Copper iodide was purchased from Aldrich. Pentamethylnickelocene was synthesized from LiCp and [NiCp*(acac)] in THF. NMR: Varian Gemini 2000 BB; Bruker AVANCE 400; The diamagnetic compounds were measured at room temperature relative to TMS. The variable temperature ^{1}H NMR spectra of the paramagnetic compound **4** were measured in a NMR Young-tube. A coaxial double NMR tube was used for Evans measurements. The inner tube was charged with the pure solvent benzene-d_6, while in the outer tube was the solvent and complex **4**. MS: Finnigan MAT 311 A (EI). Elemental analysis: CHN-O-Rapid, F. Heraeus, Zentrale Elementaranalytik, Department Chemie, Universität Hamburg.

(20) House, H. O.; Koepsell, D. G.; Campbell, W. J. *J. Org. Chem.* **1972**, *37*, 1003–1011.

1,8-(3a′,4′,7′,7a′-Tetrahydro-4′,7′-methanoindene-7a′,8′-diyl)-naphthalene (2). A Schlenk flask was charged with a solution of cyclopentadienyl lithium (3.94 g, 54.7 mmol) in THF (100 mL) and cooled to 0 °C. $ZnCl_2 \cdot$THF (12.56 g, 60.27 mmol) was added and the solution was stirred for 2 h at room temperature. A solution of 1,8-diiodonaphthalene (3.80 g, 10.0 mmol) in THF (30 mL) and copper iodide (1.78 g, 9.35 mmol) was added. After stirring for 3 days at room temperature, the reaction was quenched by pouring the reaction mixture into saturated aqueous solution of ammonium chloride. The solution was extracted with diethyl ether, dried over Na_2SO_4, filtered, and the solvent was removed. The residue was chromatographed on silica with petrol ether and gave 1.59 g (6.20 mmol, 62%) of the product as a colorless crystalline solid. ^{1}H and ^{13}C NMR data are in accordance to published data.[5d] Suitable crystals of **2** for a X-ray structure analysis were obtained from *n*-hexane solution.[6b] ^{1}H NMR (200 MHz, $CDCl_3$): δ/ppm = 7.73−7.68 (m, 1H; H-ar.), 7.66−7.61 (m, 1H; H-ar.), 7.43−7.36 (m, 3H; H-ar.), 7.27−7.21 (m, 1H; H-ar.), 6.37−6.33 (m, 1 H; H-6′), 6.30−6.25 (m, 1 H; H-5′), 5.67−5.61 (m, 1 H; H-3′), 5.27−5.33 (m, 1 H; H-2′), 3.26−3.23 (m, 1 H; H-8′), 3.22−3.11 (m, 2H; H-4′, H-1′a), 2.98−2.93 (m, 1 H; H-3a′), 2.91−2.88 (m, 1H; H-7′), 2.17-2.09 (m, 1 H, H-1′b), ^{13}C NMR (100 MHz, $CDCl_3$): δ/ppm = 145.4 (ar-quart), 139.0 (C-5′), 138.5 (ar-quart.), 133.9 (C-6′), 133.6 (ar-quart.), 131.8 (C-3′), 130.6 (ar-quart), 129.5 (C-2′), 126.5 (ar), 125.6 (ar), 125.3 (ar), 125.0 (ar), 124.2 (ar), 117.5 (ar), 66.2 (C-3a′), 64.2 (C-8′), 54.6 (C-7′), 52.2 (C-4′), 35.0 (C-7a′).

Disodium-1,8-(dicyclopentadiendi-1′-yl)-naphthalene (3). A Schlenk flask was charged with a suspension of sodium hydride (33.9 g, 1.41 mol) in decaline (270 mL). The Diels−Alder product (**2**) (2.68 g, 10.5 mmol) was added and the solution was refluxed for 2 days. The brown-green mixture was filtered and washed with hexane (3 × 50 mL) to remove decaline. The solid residue was extracted with THF (270 mL). After removing the solvent, the product was obtained as a brown powder of the disodium salt **3** (2.20 g, 7.33 mmol, 70%). ^{1}H NMR (200 MHz, THF-d_8): δ/ppm = 7.19−7.06 (m, 6 H; H-ar.), 5.75−5.67 (m, 4 H; Cp), 5.49−5.42 (m, 4 H; Cp).

1,8-Bis[(η^5-pentamethylcyclopentadienyl)(η^5-cyclopentadiendiyl)-nickel(II)]naphthalene (4). A Schlenk flask was charged with a solution of **3** (1.69 g, 5.63 mmol) in THF (35 mL). The solution was cooled to −78 °C and a solution of NiCp*(acac)[10] (1.44 g, 4.91 mmol) in THF (10 mL) was slowly added. The solution turned a reddish-brown color and was stirred for 1 day at room temperature. The solvent was removed and the residue was extracted with *n*-hexane (120 mL). The solution was restricted and stored at −25 °C for 3 days. The product precipitates in dark-red crystals (2.64 g (4.12 mmol, 84%). ^{1}H NMR (200 MHz, toluene-d_8, 25 °C, TMS, for numbering, see Figure 7 (left)) δ = 202.45, (s, 30 H, CH_3), 27.63 (s, 2H, H-3, H-m), −24.57 (s, 2H, H-4, H-p), −34.92 (s, 2H, H-2, H-o), −162.93 (s, 4H, H-2′/5′ or H-3′/4′), −173.38 (s, 4H, H-2′/5′ or H-3′/4′). MS (EI) [*m*/*z* (%)]: 640 (46) [M^+], 505 (36) [M^+ − Cp*], 446 (47) [M^+ − (Cp*Ni)], 312 (48) [M^+ − (Cp^*_2Ni)], 254 (100) [M^+ − ($Cp^*_2Ni_2$)], 239 (53). $C_{40}H_{44}Ni_2$ (642.16) calcd. C 74.81, H 6.91; found C 74.14, H 7.71.

Cyclic Voltammetry. Measurements were performed in THF with 0.4 M [*n*-Bu_4N]PF_6 as supporting electrolyte. An Amel 5000 system was used with a Pt wire as working electrode and a Pt plate (0.6 cm^2) as auxiliary electrode. The potentials were measured against Ag/$AgPF_6$ and were referenced to $E_{1/2}$(ferrocene/ferrocenium) = 0 V.

Magnetic Measurements. The magnetic susceptibility data of compound **4** were collected in a temperature range of 2−300 K under an applied field of 1 T on powdered microcrystalline samples with a SQUID magnetometer (MPMS-XL, Quantum Design). The samples were sealed in quarz tubes under vacuum. Experimental susceptibility data were corrected for the underlying diamagnetism using Pascal's constants.[18] The temperature dependent magnetic contribution of the holder was experimentally determined and subtracted from the measured susceptibility

Table 3. Crystallographic Data of the Dinuclear Complex **4**

	4
empirical formula	$C_{40}H_{44}Ni_2$
M_r [g/mol]	642.17
T [K]	153(2)
λ [pm]	71.073
crystal system	triclinic
space group	$P\bar{1}$
a [pm]	835.7(3)
b [pm]	1861.6(7)
c [pm]	2246.2(9)
α [deg]	107.100(1)
β [deg]	96.443(1)
γ [deg]	98.974(1)
V [10^6 pm^3]	3252.4(2)
Z	4
ρ_{calcd} [mg/m^3]	1.311
μ [mm^{-1}]	1.184
$F(000)$	1360
crystal size [mm]	0.50 × 0.24 × 0.14
$\theta_{min,max}$	1.73−31.00
index range	$-12 \le h \le 12$ $-26 \le k \le 26$ $-32 \le l \le 32$
reflections total	84831
reflections independent	20287
R_{int}	0.0490
reflections [$I > 4\sigma(I)$]	20287
parameters	777
GOF[a]	0.876
R_1/wR_2[b] [$I > 2\sigma(I)$]	0.0390/0.0825
R_1/wR_2[b] (all data)	0.0653/0.0879
min/max residue [e·Å^3]	−0.502/0.795

[a] GOF = goodness-of-fit = $\{\sum[w(F_o^2 - F_c^2)^2]/(n - p)\}^{1/2}$ (n = number of reflections, p = number of parameters). [b] $R_1 = \{\sum||F_o| - |F_c||\}/(\sum|F_o|)$ $wR_2 = \{\sum[w(F_o^2 - F_c^2)^2]/\sum[w(F_o^2)^2]\}^{1/2}$.

data. The resulting molar susceptibility data were plotted in χ_M vs T and $\chi_M T$ vs T. The program julx31 was used for spin Hamiltonian simulations of the data (E. Bill, Max-Planck Institute for Bioinorganic Chemistry, Mülheim, http://www.mpi-muelheim.mpg.de/bac/logins/bill/julX_en.php). For compound **4**, the magnetic data were simulated satisfactorily by using $\hat{H} = -2J_{ij}\sum \hat{S}_i \cdot \hat{S}_j$, with $\hat{S}_1 = \hat{S}_2 = 1$.

X-ray Structure Determination. The data were collected with a Bruker AXS Smart APEX CCD, Mo Kα, λ = 0.71073 Å (for crystallographic data of **4** see Table 3). The structure was solved by direct methods (SHELXS-97),[21] and the refinements on $F2$ were carried out by full-matrix least-squares techniques (SHELXL-97).[22] All non-hydrogen atoms were refined with anisotropic thermal parameters. The hydrogen atoms were refined with a fixed isotropic thermal parameter related by a factor to the value of the equivalent isotropic parameter of their carrier atoms. Weights were optimized in the final refinement cycles. CCDC-732145 (**4**) contains the supplementary crystallographic data for this paper. These data can be obtained free of charge from The Cambridge Crystallographic Data Centre via www.ccdc.cam.ac.uk/data_request/cif. Cambridge Crystallographic Data Centre (CCDC), 12 Union Road, Cambridge CB2 1EZ, UK. Phone: +44-(0)1223/336-408. Fax: +44-(0)1223/336-033. E-mail: deposit@ccdc.cam.ac.uk. Web site: http://www.ccdc.cam.ac.uk.

Computational Details. For all calculations on the density functional theory level, the program RIDFT was used.[23] Energies and geometries were developed on the unrestricted nonlocal level of theory. For geometry optimization, the energies were corrected for nonlocal exchange according to Becke[24,25] and for nonlocal correlation according to Perdew (UBP-86).[26] The def2-TZVP-split valence basis set was used for all atoms.[27] For the J_{ij}-term approximation, an additional auxiliary basis set was used.[23,28] Geometries were optimized employing restrictions to symmetry (C_2) and spin state. Calculation of force constants of the optimized structure in C_2 symmtery revealed only positive frequencies indicating the molecule to be in a minimum on the potential energy surface. For calculations of the highest symmetric state, we used a thermal occupation procedure supplied by the program revealing a quintet electronic configuration for this state. The ground state wave function was calculated using a broken symmetry approach by applying a small perturbation by an electric field in Ni−Ni direction and manual assignment of the spin−orbitals. This wave function was used for further energy and optimization procedures revealing a lower total energy.

Acknowledgment. This work was supported by the DFG—collaborative research area SFB-668. We thank E. T. K. Haupt for the measurements of the NMR spectra, the research students Sarah Puhl and Aaron G. Green for experimental work, and J. M. Manriquez for supporting information about the synthesis of Cp*Ni(acac). Dedicated to Professor Dr. Heindirk tom Dieck on the occasion of his 70th birthday.

(21) Sheldrick, G. M. *SHELXS-97 Program for crystal structure determination*; University of Göttingen, Germany, 1997.
(22) Sheldrick, G. M. *SHELXL-97 Program for crystal structure refinement*; University of Göttingen, Germany, 1997.
(23) Eichkorn, K.; Treutler, O.; Öhm, H.; Häser, M.; Ahlrichs, R. *Chem. Phys. Lett.* **1995**, *242*, 652–660.
(24) (a) Becke, A. D. *J. Chem. Phys.* **1986**, *84*, 4524–4529. (b) Becke, A. D. *J. Chem. Phys.* **1988**, *88*, 1053–1062.
(25) Becke, A. D. *Phys. Rev. A* **1988**, *38*, 3098–3100.
(26) (a) Perdew, J. P. *Phys. Rev. B* **1986**, *33*, 8822–8824. (b) Perdew, J. P. *Phys. Rev. B* **1986**, *34*, 7406.
(27) Weigend, F.; Ahlrichs, R. *Phys. Chem. Chem. Phys.* **2005**, *7*, 3297–3305.
(28) Dunlap, B. I.; Connolly, J. W. D.; Sabin, J. R. *J. Chem. Phys.* **1979**, *71*(12), 4993–4999.